

Supporting Information

Cu-organic framework-derived V-doped carbon nanostructures for organic dye removal

Xiao-Sa Zhang,^a Hong-Tian Zhao,^a Yu Liu,^a Wen-Ze Li,^{a*} Ai-Ai Yang^a and Jian Luan^{b*}

^a College of Sciences, Shenyang University of Chemical Technology, Shenyang, 110142, P. R. China

^b College of Sciences, Northeastern University, Shenyang, 100819, P. R. China

E-mail: liwenze@syuct.edu.cn (W. Z. Li); 2010044@stu.neu.edu.cn (J. Luan)

Table S1 Crystallographic data for complex 1

Complex	1
Formula	C ₂₈ H ₂₂ Cu ₃ O ₁₄
Formula wt	773.08
Crystal system	Monoclinic
Space group	P 21/c
T (K)	296(2)
a (Å)	5.9687(4)
b (Å)	29.7669(18)
c (Å)	7.6708(5)
α (°)	90
β (°)	93.6970(10)
γ (°)	90
V (Å ³)	1360.03(15)
Z	2
D _{calc} (g cm ⁻³)	1.888
F(000)	778
θ _{max} (°)	26.51
R _{int}	0.0374
R ₁ ^a [I > 2σ(I)]	0.0436
wR ₂ ^b (all data)	0.1142
GOF	1.031

^a $R_1 = \sum ||F_o| - |F_c|| / \sum |F_o|$, ^b $wR_2 = \sum [w(F_o^2 - F_c^2)^2] / \sum [w(F_o^2)^2]^{1/2}$.

Table S2 Selected bond distances (\AA) and angles ($^\circ$) for complex **1**.

Cu(1) - O(6)	1.914(4)	O(1W) - Cu(2)	1.945(4)
Cu(1) - O(6)#1	1.914(4)	Cu(2) - O(3)	1.905(4)
Cu(1) - O(2)#1	1.955(4)	Cu(2) - O(6)	1.969(4)
Cu(1) - O(2)	1.955(4)	Cu(2) - O(6)#2	2.091(4)
O(1) - Cu(2)	2.122(4)	O(6) - Cu(1) - O(6)#1	180
O(6) - Cu(1) - O(2)#1	88.54(17)	O(3) - Cu(2) - O(6)#2	143.01(18)
O(6)#1 - Cu(1) - O(2)#1	91.46(17)	O(1W) - Cu(2) - O(6)#2	91.49(17)
O(6) - Cu(1) - O(2)	91.46(17)	O(6) - Cu(2) - O(6)#2	81.52(15)
O(6)#1 - Cu(1) - O(2)	88.53(17)	O(3) - Cu(2) - O(1)	130.62(19)
O(2)#1 - Cu(1) - O(2)	179.998(2)	O(1W) - Cu(2) - O(1)	90.26(15)
O(3) - Cu(2) - O(1W)	92.84(18)	O(6) - Cu(2) - O(1)	92.00(16)
O(3) - Cu(2) - O(6)	91.13(17)	O(6)#2 - Cu(2) - O(1)	86.04(17)
O(1W) - Cu(2) - O(6)	172.49(18)		

Symmetry codes: #1 $-x + 1, -y + 1, -z + 1$; #2 $-x, -y + 1, -z + 1$.

Table S3 BET surface areas, pore volumes and pore sizes of synthesized carbon nanostructures.

Samples	Surface Area			Pore Volume		Pore Size
	BET Surface Area ($\text{m}^2 \text{ g}^{-1}$)	Micropore Area ($\text{m}^2 \text{ g}^{-1}$)	External Surface Area ($\text{m}^2 \text{ g}^{-1}$)	Total pore volume ($\text{cm}^3 \text{ g}^{-1}$)	Micropore volume ($\text{cm}^3 \text{ g}^{-1}$)	Adsorption average pore width (nm)
C-1-600	33.13	21.36	11.77	0.0922	0.0115	11.13
C-1	58.42	54.47	46.87	0.5678	0.0259	19.44
C-1-1000	44.79	32.47	12.32	0.1675	0.0173	14.96
C-Mo-1	76.42	48.37	28.05	0.1853	0.0259	9.7
C-W-1	80.95	38.44	42.51	0.2001	0.0207	9.89
C-S-1	82.63	71.41	11.22	0.3509	0.0359	16.99
C-V-600	40.11	20.87	19.24	0.1579	0.011	15.75
C-V-1	84.18	82.49	71.36	0.6467	0.0351	15.36
C-V-1000	69.03	50.77	18.25	0.1766	0.0272	10.23

Table S4 Organic dyes with different charge types and sizes.

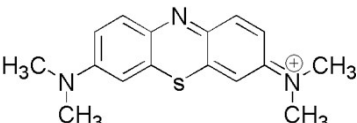
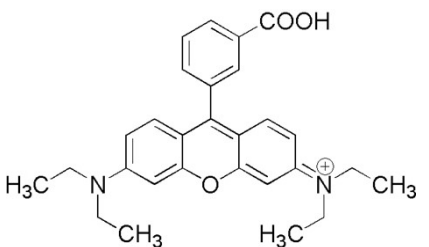
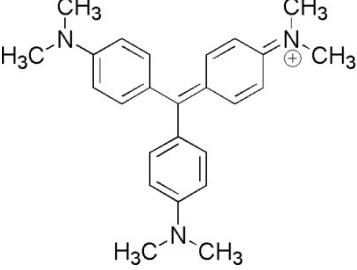
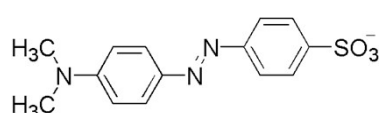
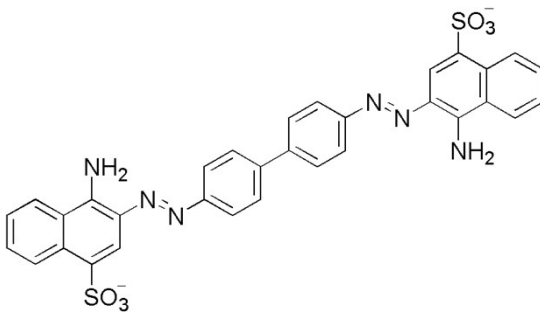
Dye	Formula	Charge type	Size (nm × nm × nm)
Methylene Blue (MB)		Cationic	0.40 × 0.79 × 1.63
Rhodamine B (RhB)		Cationic	0.68 × 1.18 × 1.57
Gentian Violet (GV)		Cationic	0.40 × 1.30 × 1.37
Methyl Orange (MO)		Anionic	0.53 × 0.73 × 1.74
Congo Red (CR)		Anionic	0.39 × 0.86 × 2.61

Table S5 Thermodynamic parameters at different temperatures.

Dye	T (K)	ΔG (kJ mol ⁻¹)	ΔH (kJ mol ⁻¹)	ΔS (kJ mol ⁻¹ K ⁻¹)
MB	298	-7.094	1.180	0.028
	303	-7.233		
	313	-7.511		
	323	-7.788		
RhB	298	-6.666	0.791	0.025
	303	-6.791		
	313	-7.041		
	323	-7.291		
GV	298	-7.182	1.881	0.030
	303	-7.334		
	313	-7.639		
	323	-7.943		
MO	298	-4.788	0.933	0.019
	303	-4.884		
	313	-5.075		
	323	-5.267		
CR	298	-5.040	0.408	0.018
	303	-5.131		
	313	-5.314		
	323	-5.497		

Table S6 Pseudo-first-order kinetic parameters for the photodegradation of CR by C-V-1.

Dye	Concentration (mg L ⁻¹)	Rate Constant k (min ⁻¹)	Half-life $t_{1/2}$ (min)	R^2
MB	10	0.0067	103.61	0.7943
RhB	10	0.0060	115.91	0.9354
GV	10	0.1080	6.42	0.9586
MO	40	0.0051	135.65	0.9326
CR	80	0.0052	134.07	0.9710

Table S7 Comparison of the adsorption and photocatalytic capacities and rates of variety dyes by C-V-1.

Dye	Concentration (mg L ⁻¹)	Adsorption capacity (mg g ⁻¹)	Adsorption rate (%)	Degradation capacity (mg g ⁻¹)	Degradation rate (%)
MB	10	174.13	87.07	176.28	88.14
RhB	10	147.06	73.53	159.60	79.80
GV	10	179.92	89.96	198.02	99.01
MO	10	137.96	68.98	142.62	71.31
CR	10	132.96	66.48	143.82	71.19

Table S8 Comparison of the adsorption/photodegradation efficiencies with other V-contained materials.

Material	Dye	Type	Equilibrium time (min)	Material Weigh (mg)	C ₀ (mg L ⁻¹)	Degradation rate (%)	q _{max} (mg g ⁻¹)	Ref.
V-doped CaTiO ₃	MB	Photodegradation	120	100	10	94	—	S1
V-doped WO ₃	MB	Photodegradation	120	10	10	66	—	S2
V-doped WO ₃	RhB	Photodegradation	180	40	150	93	—	S3
V-modified N/Si co-doped TiO ₂	MB	Photodegradation	360	10	0.05	90	—	S4
Ni-doped V ₂ O ₅	RhB	Photodegradation	150	50	0.1	100	—	S5
V-supported CoFe ₂ O ₄ chitosan-V-Ti-magnetite composite	MB	Photodegradation	8	15	0.1	100	—	S6
Fe@V-carbon nanofiber	CR	Adsorption	2880	80	100	—	90	S7
[Zn ₃ (4-atrz) ₆ V ₆ O ₁₈] [·] 4H ₂ O	MO	Photodegradation	10	10	20	90	—	S8
atrz = amino-1,2,4-triazole	RhB	Photodegradation	20	10	20	100	—	
[Ag ₄ (Hpytz) ₂ (H ₂ pytz)][HVW ₁₂ O ₄₀] [·] 3H ₂ O	MB	Photodegradation	180	150	10	76	—	S9
H ₂ pytz = 5'-{(pyridin-4-yl)-1H,2'H-3,3'-bi(1,2,4-triazole)}	MO	Photodegradation	180	150	10	19	—	
[V ₂ O ₆ Zn(4-dpye)] _n	MB	Photodegradation	210	50	10	58	—	
4-dpye = N,N'-bis(4-pyridinecarboxamide)-1,2-ethane	RhB	Photodegradation	210	50	3	40	—	S10
C-V-1	MB	Photodegradation	90	150	10	93	—	
	RhB	Photodegradation	90	150	10	37	—	S11
	MB	Adsorption	240	5	10	—	170	
	RhB	Adsorption	240	5	10	—	145	
	GV	Adsorption	240	5	10	—	175	
	MO	Adsorption	240	5	40	—	273	
	CR	Adsorption	240	5	80	—	605	This work
	MB	Photodegradation	240	5	10	88	—	
	RhB	Photodegradation	240	5	10	79	—	
	GV	Photodegradation	240	5	10	99	—	
	MO	Photodegradation	240	5	40	71	—	
	CR	Photodegradation	240	5	80	71	—	

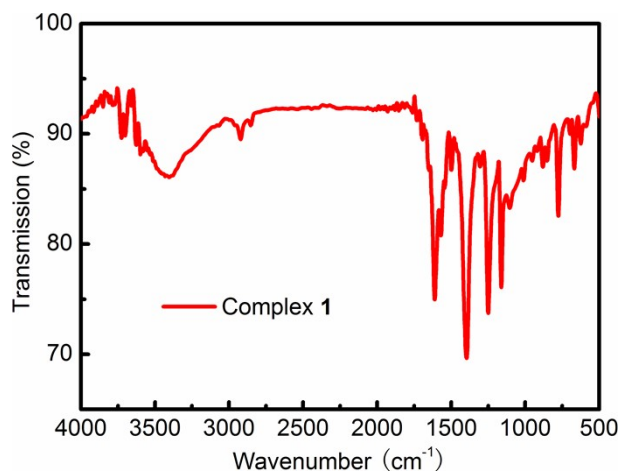


Figure S1 The IR spectrum of complex 1.

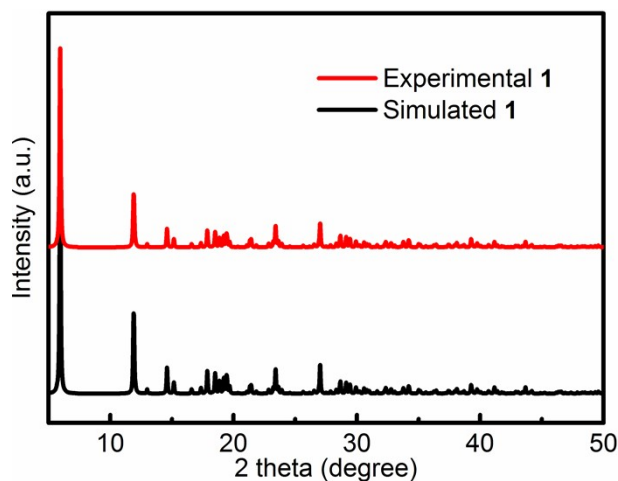


Figure S2 The PXRD patterns of simulated and fresh sample for complex 1.

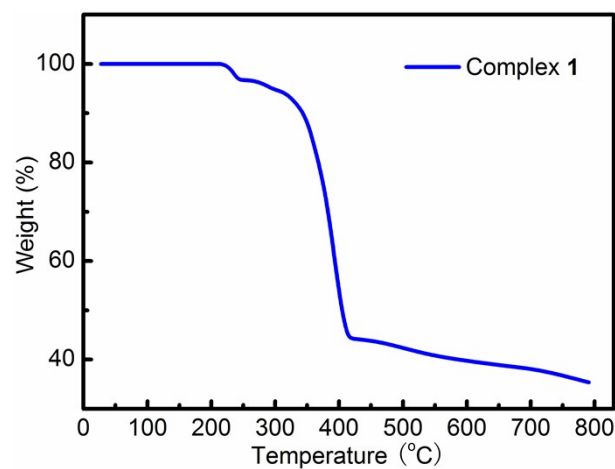


Figure S3 The TG curve of complex 1.

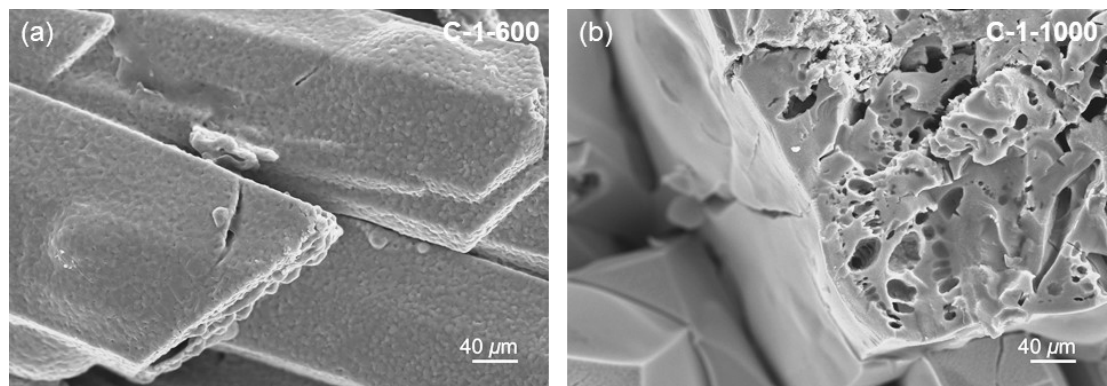


Figure S4 SEM images of **C-1-600** (a) and **C-1-1000** (b).

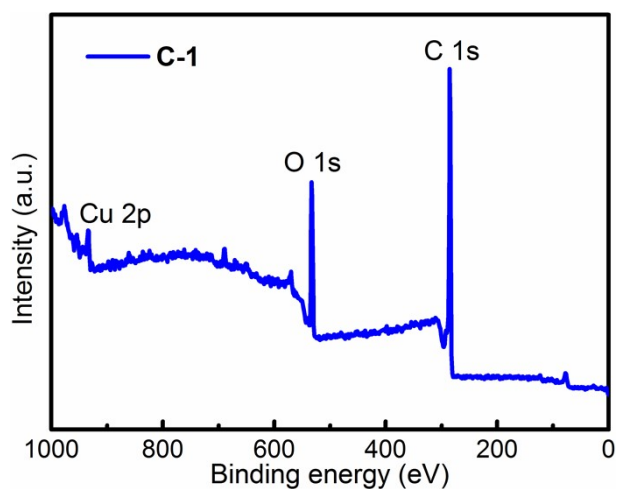


Figure S5 XPS spectrum of **C-1**.

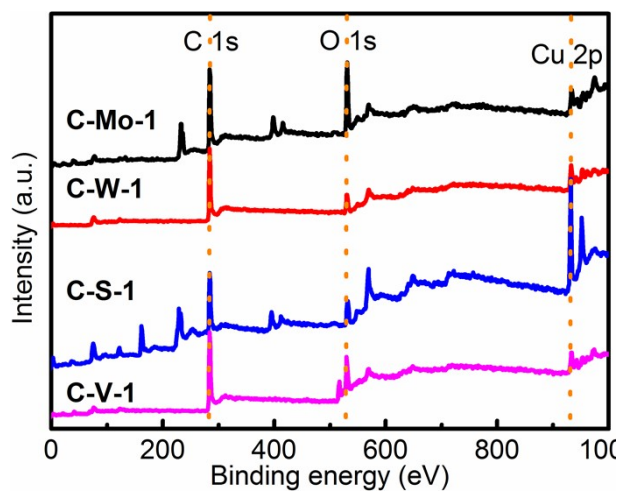


Figure S6 XPS spectra of **C-Mo-1**, **C-W-1**, **C-S-1** and **C-V-1**.

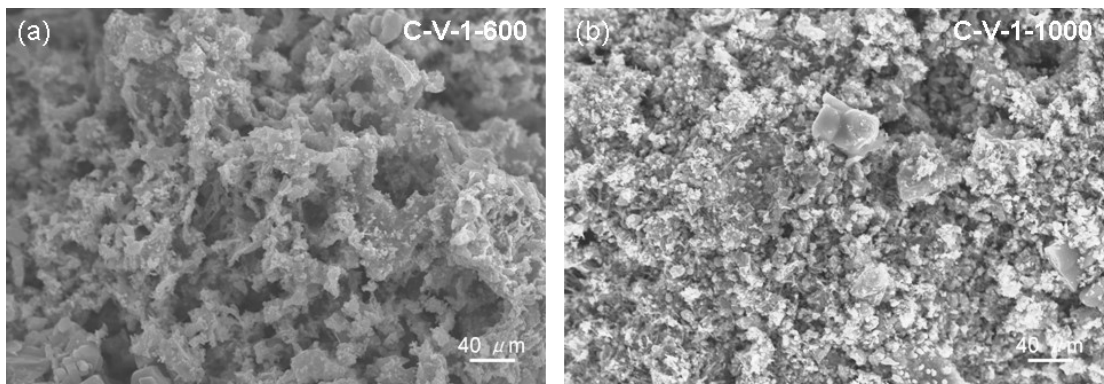


Figure S7 SEM images of **C-V-1-600** (a) and **C-V-1-1000** (b).

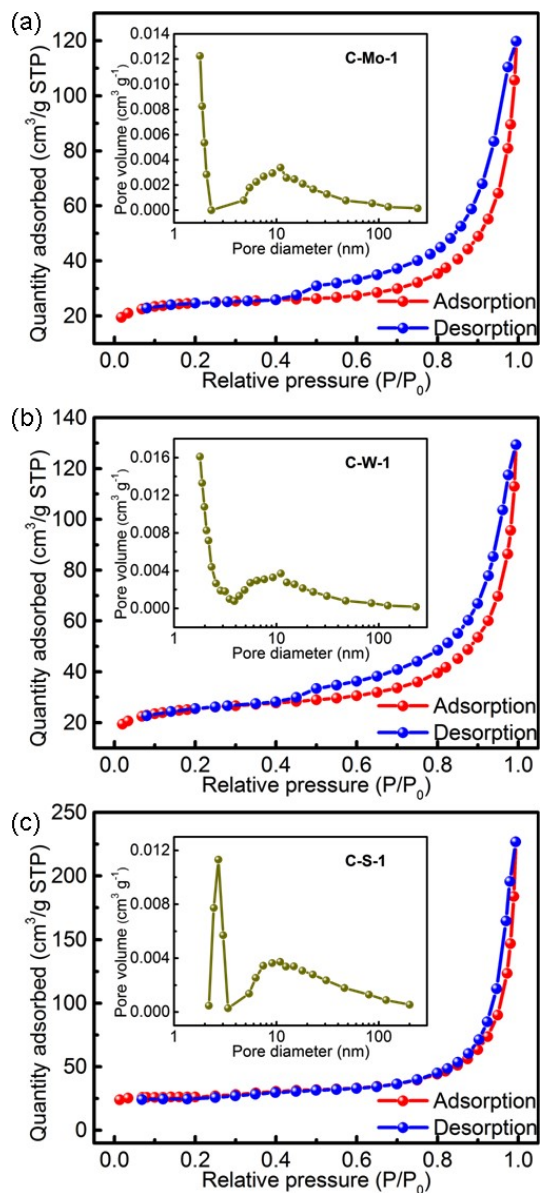


Figure S8 Nitrogen adsorption and desorption isotherms (Insert: the pore size distribution) of **C-Mo-1** (a), **C-W-1** (b) and **C-S-1** (c).

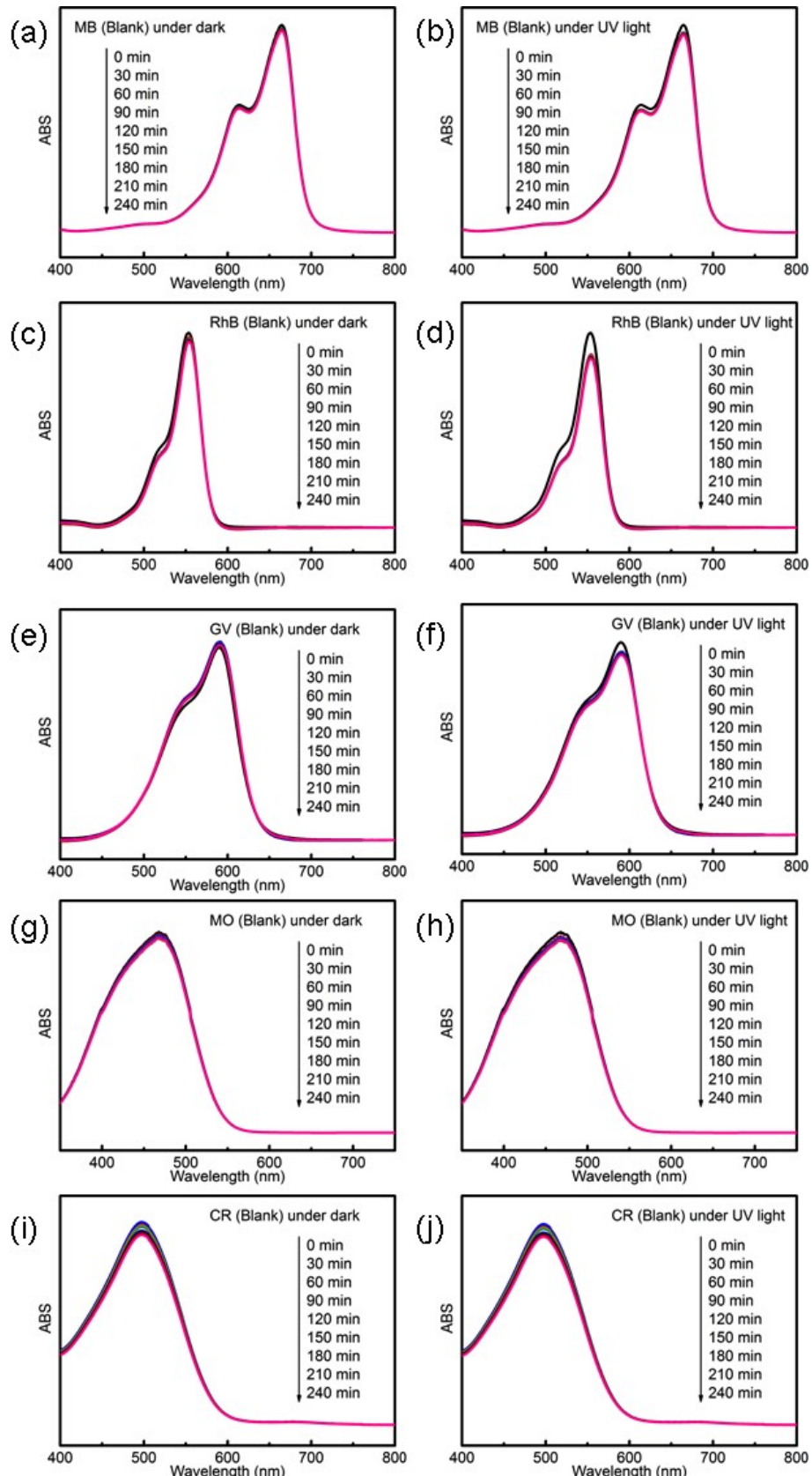


Figure S9 UV-vis spectra of blank experiment for dye adsorption and photocatalysis (performed in the absence of any catalyst).

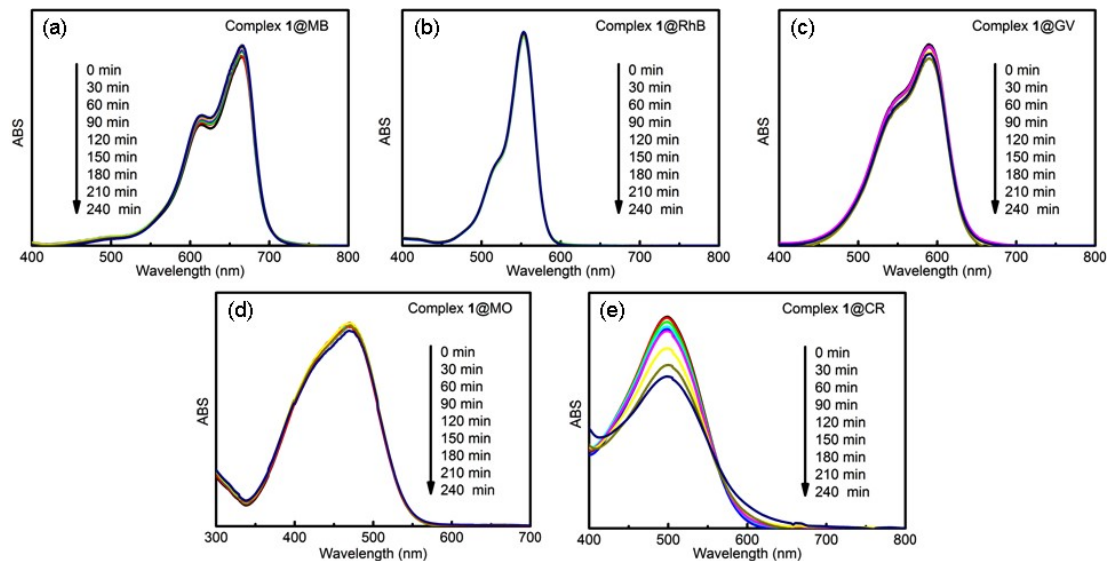


Figure S10 UV-vis spectra of MB (a), RhB (b), GV (c), MO (d) and CR (e) solutions recorded after different adsorption times with complex **1**.

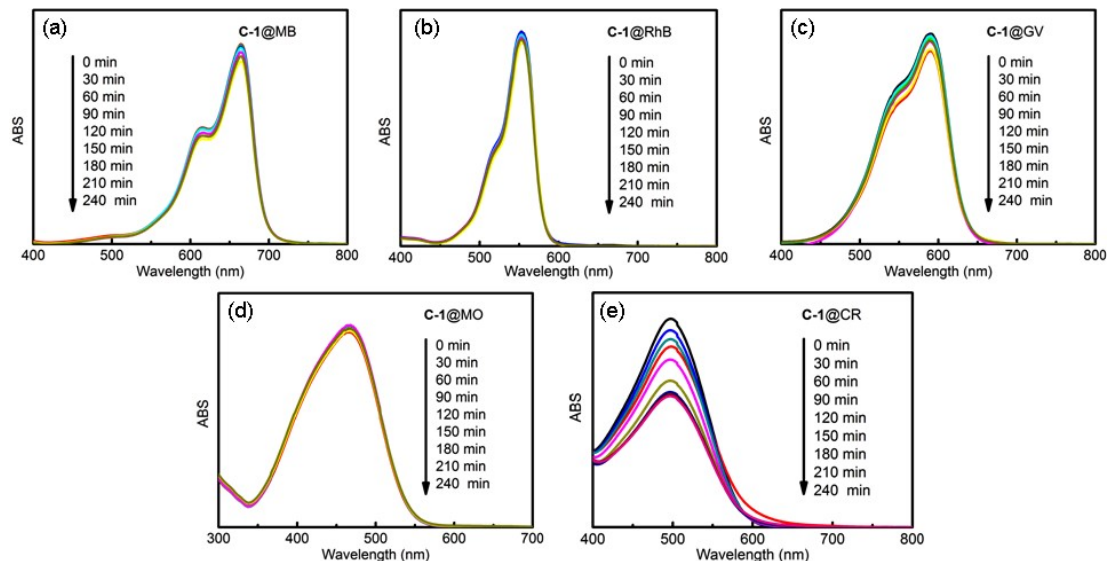


Figure S11 UV-vis spectra of MB (a), RhB (b), GV (c), MO (d) and CR (e) solutions recorded after different adsorption times with **C-1**.

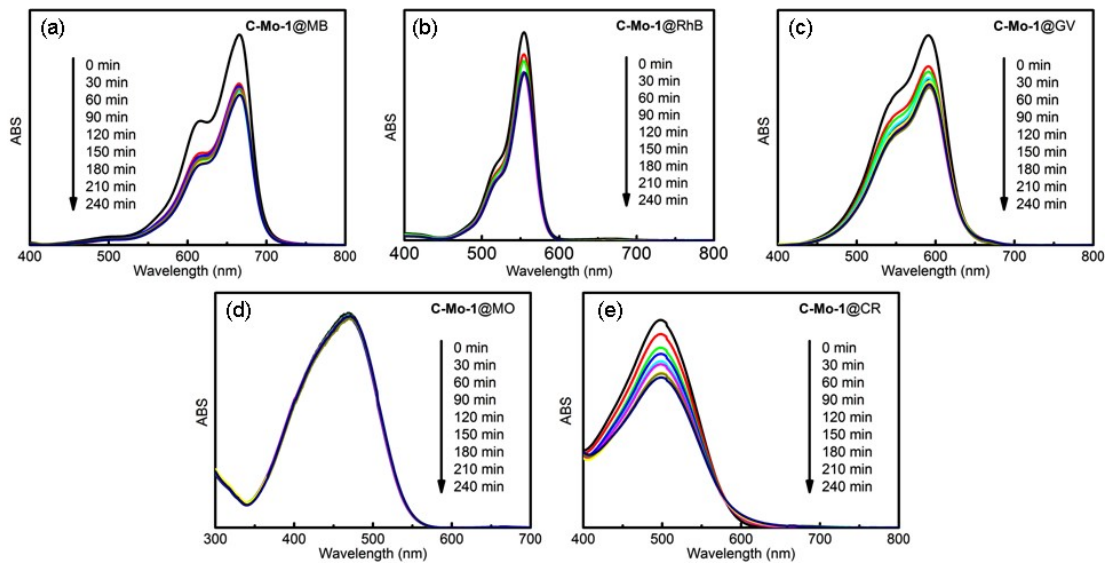


Figure S12 UV-vis spectra of MB (a), RhB (b), GV (c), MO (d) and CR (e) solutions recorded after different adsorption times with **C-Mo-1**.

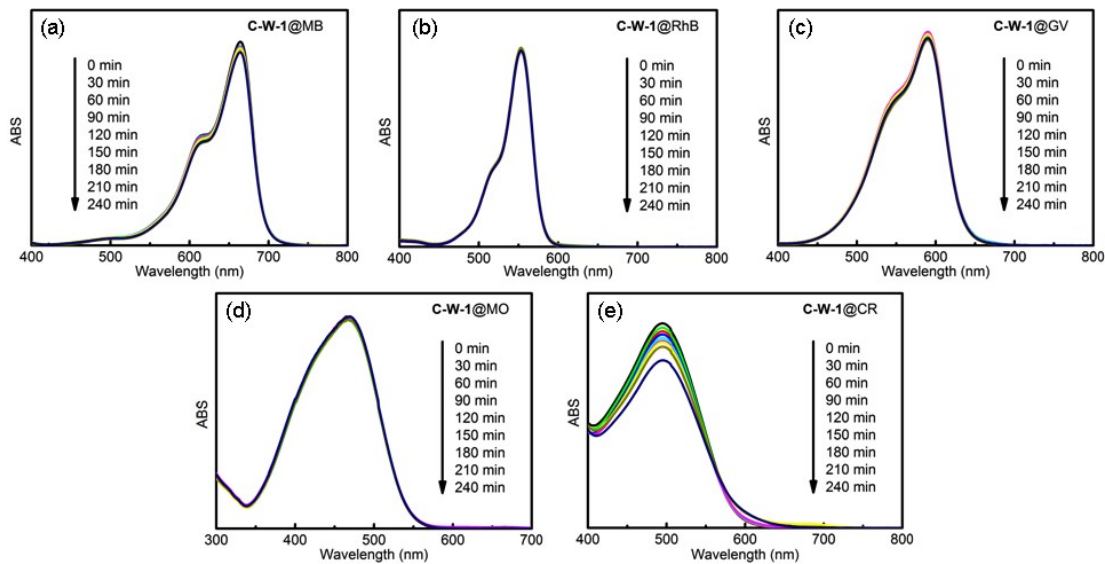


Figure S13 UV-vis spectra of MB (a), RhB (b), GV (c), MO (d) and CR (e) solutions recorded after different adsorption times with **C-W-1**.

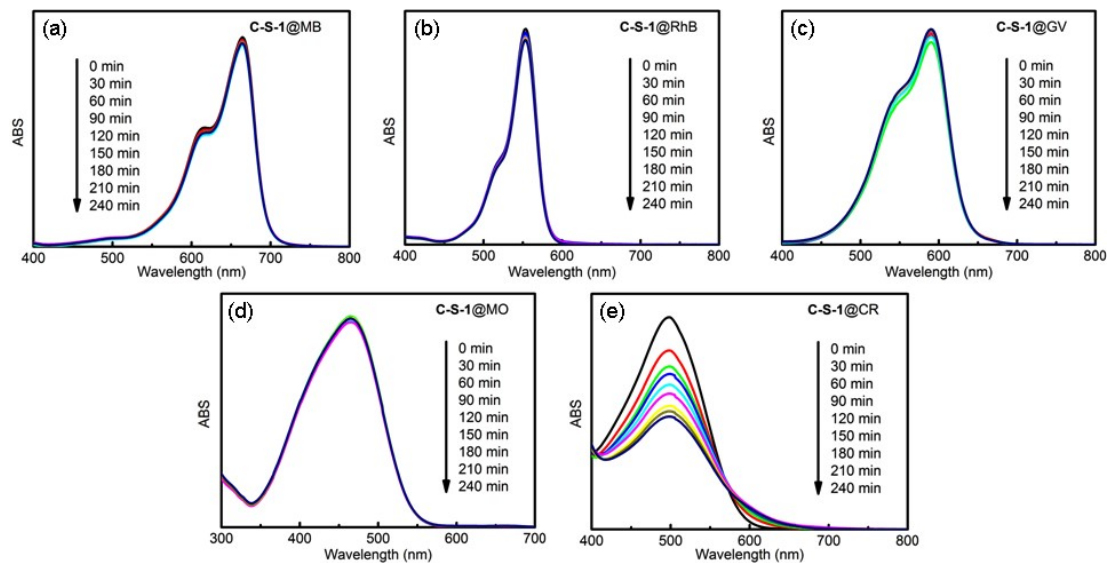


Figure S14 UV-vis spectra of MB (a), RhB (b), GV (c), MO (d) and CR (e) solutions recorded after different adsorption times with **C-S-1**.

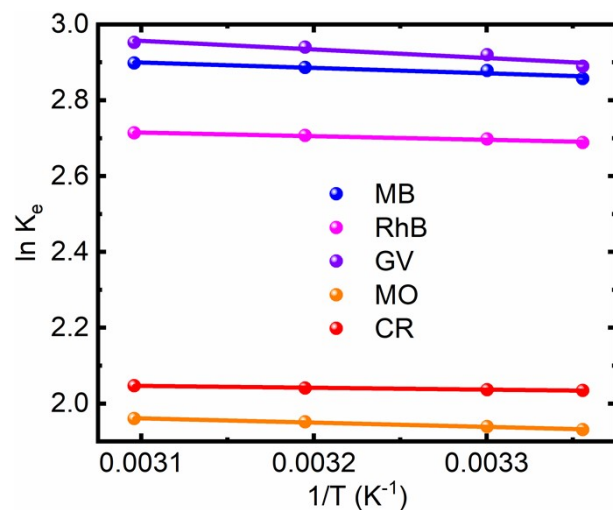


Figure S15 The plot of $\ln K_e$ - $1/T$ for adsorption of MB, RhB, GV, MO and CR on **C-S-1**.

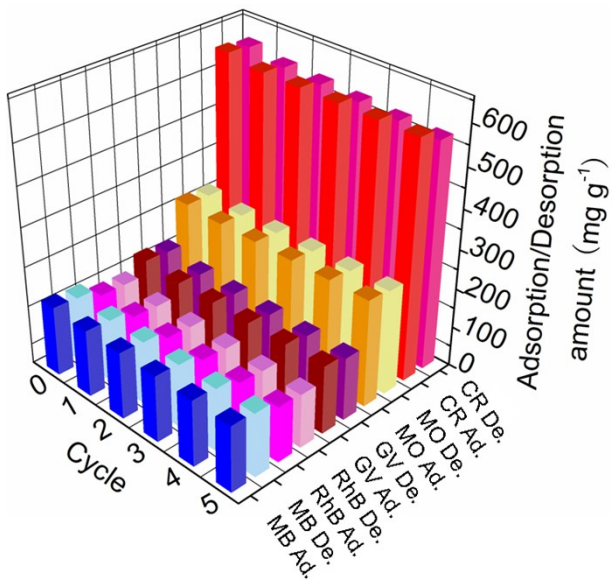


Figure S16 The cycling stability of the adsorption/desorption of dyes on the **C-V-1**.

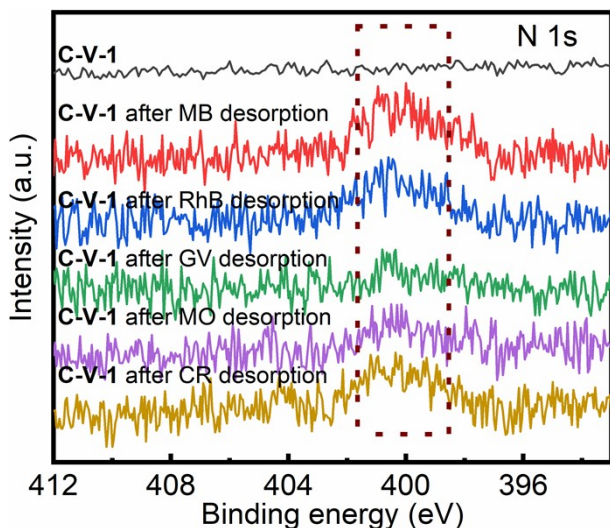


Figure S17 XPS analysis of the N1s spectra for **C-V-1** and **C-V-1** after different dyes desorption.

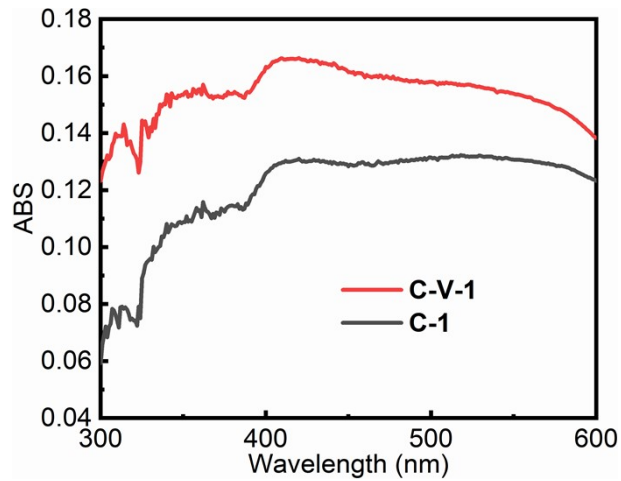


Figure S18 Diffuse-reflectance spectra of **C-1** and **C-V-1** matrials.

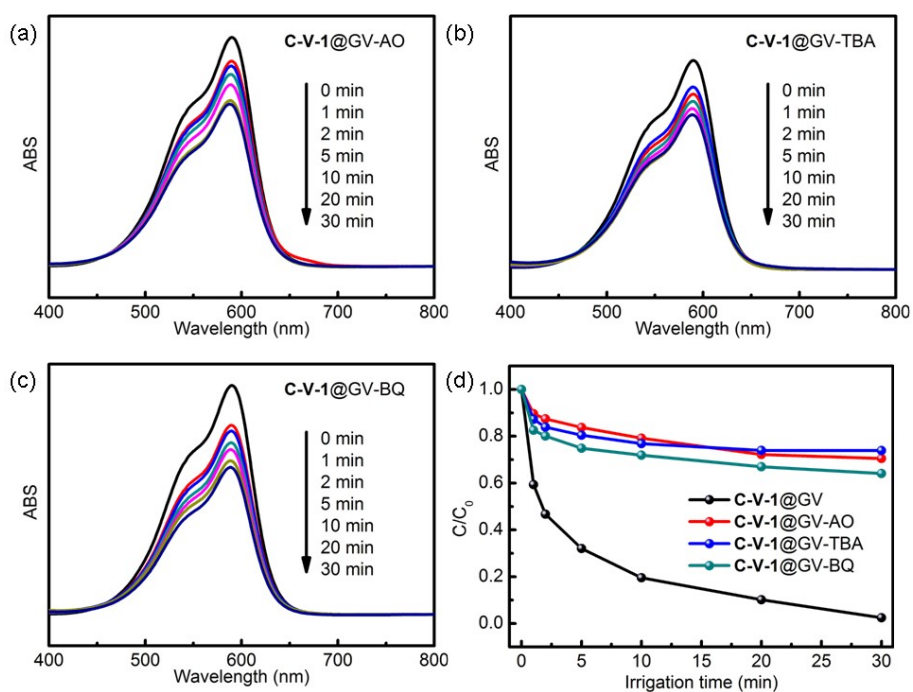


Figure S19 UV-vis spectra of GV solution on the **C-V-1** in presence of AO (a), TBA (b) and BQ (c). (d) The photodegradation rates of GV on the **C-V-1** in presence of various scavengers.

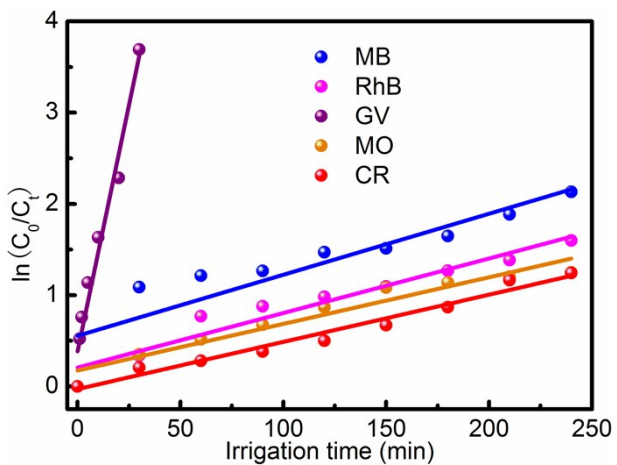


Figure S20 Pseudo-first-order plots with respect to time for **C-V-1** in aqueous dye solutions.

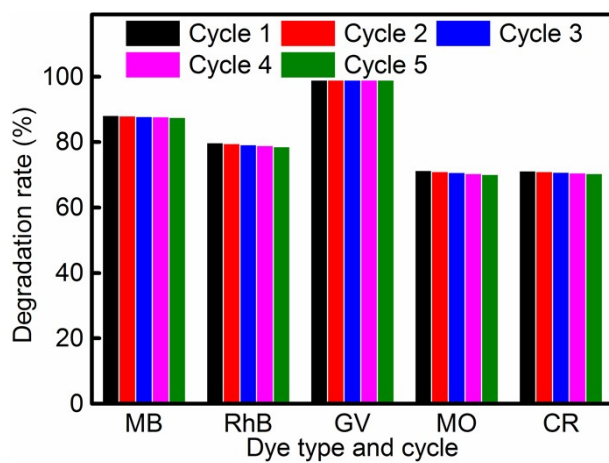


Figure S21 The reproducibility of the photocatalyst **C-V-1**.

References

- S1 H. Bantawal, U. S. Shenoy and D. K. Bhat, *Nanoscale Adv.*, 2021, **3**, 5301–5311.
- S2 C. W. Yeh, C. H. Hung, K. R. Wu and C. C. Yang, *Environ. Eng. Sci.*, 2014, **31**, 42–48.
- S3 A. J. Antony, S. M. J. Kala, C. Joel, R. B. Bennie and S. J. Praveendaniel, *Phys. Chem. Solids*, 2021, **157**, 110169.
- S4 A. Mase, T. Sugita, M. Mori, S. Iwamoto, T. Tokutome, K. Katayama and H. Itabashi, *Chem. Eng. J.*, 2013, **225**, 440–446.
- S5 M. Rafique, M. Hamza, M. Shakil, M. Irshad, M. B. Tahir and M. R. Kabli, *Appl. Nanosci.*, 2020, **10**, 2365–2374.
- S6 R. Salami, M. Amini, M. Bagherzadeh and H. Hosseini, *Appl. Organometal. Chem.*, 2019, **33**, e5127.
- S7 W. Zhang, Y. Y. Lan, M. T. Ma, S. Y. Chai, Q. T. Zuo, K. H. Kim and Y. Q. Gao, *Environ. Int.*, 2020, **142**, 105798.
- S8 A. A. Taha, A. A. Hriegz, Y. N. Wu, H. T. Wang and F. T. Li, *J. Colloid Interface Sci.*, 2014, **417**, 199–205.
- S9 X. L. Wang, C. H. Gong, J. W. Zhang, L. L. Hou, J. Luan and G. C. Liu, *CrystEngComm*, 2014, **16**, 7745–7752.
- S10 X. L. Wang, L. F. Chen, G. C. Liu, J. Luan, J. J. Cao, C. H. Gong and Z. H. Chang, *Inorg. Chem. Commun.*, 2015, **53**, 64–67.
- S11 X. L. Wang, J. J. Sun, H. Y. Lin, Z. H. Chang and G. C. Liu, *Inorg. Chem. Commun.*, 2016, **73**, 152–156.